Synchronization patterns in rings of locally coupled Kuramoto oscillators

Ph.D. thesis summary

A DISSERTATION PRESENTED
BY
KÁROLY DÉNES
TO
THE FACULTY OF PHYSICS

FOR THE DEGREE OF
DOCTOR OF PHILOSOPHY
IN
PHYSICS
THESIS ADVISOR: PROF. DR. ZOLTÁN NÉDA

BABEŞ-BOLYAI UNIVERSITY
CLUJ-NAPOCA, ROMANIA
NOVEMBER 2020

Thesis advisor: Prof. Dr. Z. Néda Károly Dénes

Abstract

This thesis investigates pattern formation in ensembles of locally coupled Kuramoto rings. Although this topic is well documented in the literature, we revisited the problem from different perspectives. Throughout our analysis we have focused on emergent phase-locked states, where oscillators end up having the same frequency, also allowing a constant non-vanishing phase difference between each first order neighbor. Starting from a fairly simple system of homogeneous oscillators with uniform one dimensional coupling topology we have identified all types of phase locked states analytically. The dynamics was also investigated in order to correlate random phase initial states with the ordered final states. The possibilities of predicting final states from disordered initial states have been discussed and two types of prediction methods were introduced. The performance of these methods have been compared in the case of homogeneous oscillators and heterogeneous systems as well. As a next step we have generalized our systems of interest by introducing a constant uniform time delay in the interaction, increasing thus the dimensionality of the problem. Our aim was to determine the effect of the delay on the stability and attraction basin sizes of the phase locked states. We found that both the local stability and basin sizes depend strongly on the relevant system parameters, resulting in a very different picture compared to the non-delayed case. Since time delayed systems are equivalent to infinite dimensional systems we briefly discuss the possibility of obtaining other types of attractors as well.

KEYWORDS: self-organization, spontaneous synchronization, coupled oscillators, phase blocking, Kuramoto model, final state prediction, attraction basins, time delay

Contents of the Ph.D. thesis

Contents of the summary

1 Introduction

Spontaneous synchronization[1] is an intriguing phenomena present in different fields of sciences ranging from biology (synchronous flashing of fireflies[2], pacemaker cells[3] etc.) to engineering (collective behavior of Josephson junctions arrays[4], the case of the Millennium Bridge[5] etc). The first recorded observation of spontaneous synchronization is from the 17th century dutch physicist Christiaan Huygens who described the synchronization of two pendulum clocks hanging from the same suspension rod, which he called as "odd sympathy"[6]. The next milestone came in 1958, when Norbert Wiener observed a strong activity in human brain waves in the low frequency domain called alpha rythm.[7]. He hypothesized that there are oscillators in the brain with slightly different natural frequencies, which interact with each other by "frequency pulling", leading to a more precise collective oscillation. A more elaborate description of emerging order in biological oscillators came from a theoretical biologist named Arthur Winfree in 1967[8]. He introduced the phase model approximation of oscillators. In his simple model the oscillators had different natural frequencies and each oscillator was coupled to all the other ones. This simple model uncovered intriguing similarities between spontaneous synchronization and order-disorder type thermodynamic phase-transitions. Inspired by the work of Winfree, a physicist named Yoshiki Kuramoto introduced an analytically solvable model of coupled phase oscillators in 1975 which is capable to analitically reproduce similar results[9]. He also considered an ensemble of non-identical phase oscillators, with a unimodal intrinsic frequency distribution. For measuring the degree of order in the system, Kuramoto introduced a complex valued order parameter. Using intuitive assumptions and self-consistency, Kuramoto was able to show that in the thermodynamic limit there is a critical coupling strength above which partially synchronized states begin to appear. In spite that the problem seems to be solved, his derivation raised serious question as well[10,11].

The Kuramoto model triggered many new studies in the field of statistical physics and nonlinear dynamics. Soon it became the fundamental tool in studying and modeling complex behavior. With the sharp growth of computational power, numerical experiments studying collective behavior quickly gained new perspectives. The modularity of the oscillators enables to implement and investigate systems having almost arbitrary type of interaction topology[12,13]. Advances in network science around the new

millennium[14,15] motivated studies on the Kuramoto model considering local interaction on complex networks[16–20]. New variants of the Kuramoto model have also appeared considering disorder in coupling constants[21], frustration[22], noise[23] and external fields[24] as well. In 2002, Kuramoto with his colleague Battogtokh discovered a state in non-locally coupled oscillators in which disordered and ordered regimes coexist[25], a phenomenon later called as chimera states[26]. Since then chimera states became one of the most active field of nonlinear dynamics, opening up new challanges to the celebrated model. Experimental studies revealed even more new possibilities for chimera states to emerge[27–31]. Remote synchronization, another novel form of complex behavior, has also been confirmed in Kuramoto-type systems[32,33]. During the past four and a half decades numerous varieties of the Kuramoto model were studied targeting different problems.

In the thesis we summarize our findings on systems of one-dimensional locally coupled Kuramoto oscillators. Chapter 2 of the thesis reviews our results on non-delayed rings discussing the results published in Communications in Nonlinear Science and Numerical Simulation[34] and Romanian Reports in Physics[35]. In these works we focused mainly on homogeneous oscillators and their phase locked states. We determined all possible phase locked states and their linear stability using a novel framework. The dynamics of such ensembles have been studied and the problem of predictability of the final states has been examined. The results presented here shed light also on the relevant time scales in such rings. We show that under certain circumstances our results on homogeneous oscillators can be applied on heterogeneous systems as well. In Chapter 3 we present our studies on Kuramoto rings with delayed coupling. Using time rescaling we were able to construct the stability map of the system which exhibits high level of symmetry and periodicity. Besides linear stability we studied the changes in attraction basin sizes due to variations of the system parameters. The results presented here were also published in the journal Communications in Nonlinear Science and Numerical Simulation[36]. An outlook chapter concludes the thesis giving new research ideas and further questions to be addressed in locally coupled oscillator systems.

2

Locally coupled Kuramoto oscillators without time delay in the interactions

2.1 Emergent patterns

The systems we studied consist of a system of N first order ordinary differential equations, coupled through a sinusoidal kernel[37–39]:

$$\dot{\theta}_i = \omega_0 + K[\sin(\theta_{i-1} - \theta_i) + \sin(\theta_{i+1} - \theta_i)]\,, \quad i = \overline{1, N}\,, \tag{2.1}$$

N is the number of oscillators and θ_i is the phase of oscillator having index i. The natural frequency ω_0 is the same for each oscillator and the positive real number K is the uniform coupling constant. In order to maintain a ring-like structure periodic boundary conditions are applied: $\theta_0 = \theta_N$ and $\theta_{N+1} = \theta_1$. In order the get a homogeneous differential equation we switch to a rotating reference frame:

$$u_i(t) = \theta_i(t) - \omega_0 t\,. \tag{2.2}$$

The transformation will yield the following system of equations in the $u_i(t)$ variables:

$$\dot{u}_i = K[\sin(u_{i-1} - u_i) + \sin(u_{i+1} - u_i)] = F(u_{i-1}, u_i, u_{i+1})\,. \tag{2.3}$$

It can be shown that such a system is a gradient system, where the equations of motions can be derived from a potential function as $\dot{u}_i = -\partial V/\partial u_i$[40]. The advantage of a gradient system is that the allowed asymptotic states are fixpoints, while limit cycles and chaotic attractors can not appear[41]. This means that the fixpoints correspond to the stationary points of the potential function, which can be of three types: minimum, saddle, or maximum point.

In a fixpoint the system does not change its state, thus we search for these points by taking $\dot{u}_i = 0$. For a triplet of oscillators (u_{i-1}, u_i and u_{i+1}) this can be achieved in either of the two cases:

$$u_{i+1} - 2u_i + u_{i-1} = 2k_i\pi, \quad k_i \in \mathbb{Z}, \tag{2.4}$$

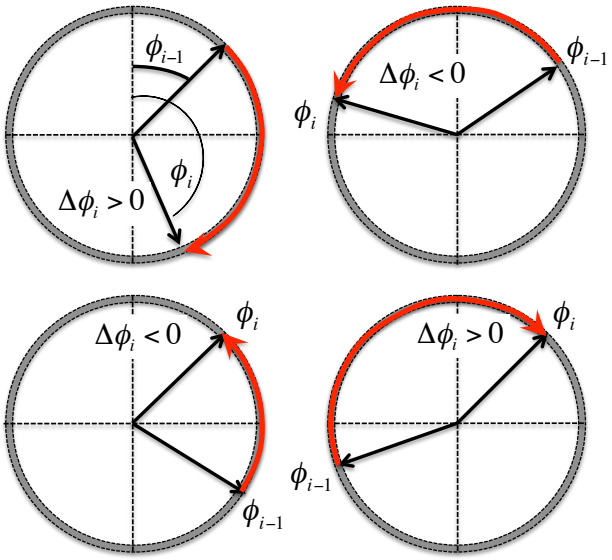

Figure 2.1: Illustration of the $\Delta\phi_i$ phase shift defined in Eq. (2.7).

or:

$$u_{i+1} - u_{i-1} = (2q_i + 1)\pi, \quad q_i \in \mathbb{Z}. \tag{2.5}$$

Since there are N such triplets and for each triplet one of the above two condition has to be true, there are many ways to construct a fixpoint where all time derivatives are zero. In order to separate these different cases we distinguish three classes of stationary states:

(a) condition (2.4) holds for all i values,

(b) condition (2.5) is fulfilled for all i indeces,

(c) for some i condition (2.4) is true and for the remaining pairs condition (2.5) holds.

Both (a) and (b) cases lead to symmetric states at the level of triplets of oscillators, while class (c) states allow unbalanced triplets to appear, corresponding to a nontrivial symmetry breaking.

We transform the u_i values in order to obtain phases between 0 and 2π:

$$\phi_i = u_i \bmod 2\pi. \tag{2.6}$$

Now we introduce a $\Delta\phi_i$ parameter called as *phase shift* for representing the relative position of oscillator pairs. It is equivalent to a signed distance measure on the perimeter of a unit circle, having values between $-\pi$ and π. The phase shift is calculated using the floor function ($\lfloor x \rfloor$):

$$\Delta\phi_i = (\phi_i - \phi_{i-1}) - 2\pi \left\lfloor \frac{\phi_i - \phi_{i-1} + \pi}{2\pi} \right\rfloor. \tag{2.7}$$

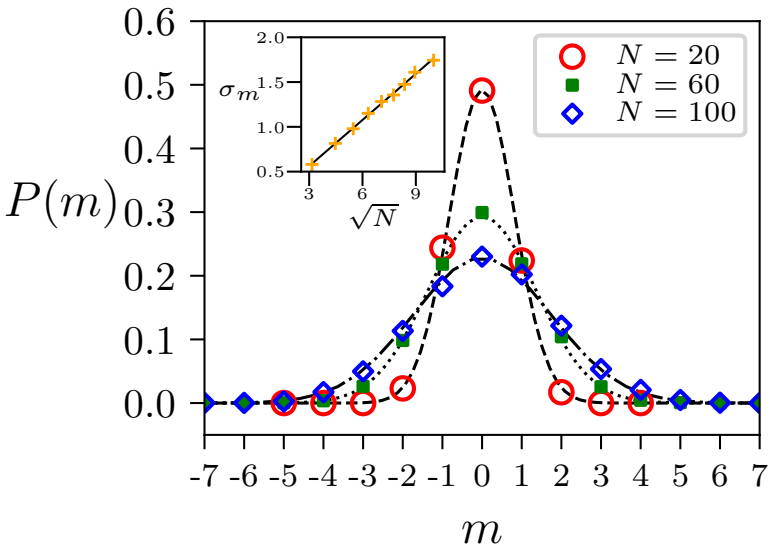

Figure 2.2: Probability distribution of attractors for increasing system sizes. Gaussian envelope curves are fitted over the discrete distributions. The $P(m)$ probabilities are proportional to the size of each attractor's attraction basin. The inset shows the scaling of the spread of the distributions as a function of the square root of N, namely $\sigma_m \propto \sqrt{N}$. Each distributions was constructed considering an ensemble of 5000 random initial states. $K = 1.5$, $\omega_0 = 2$.

A more comprehensive visual representation of this definition is presented on Fig. 2.1. As the figure shows $\Delta\phi_i$ is simply the shortest path between the tips of two successive vectors along the perimeter of the unit circle. The sign is positive when the advance from $i-1$ to i is clockwise and negative if counter-clockwise. In order to rule out the ambiguity at $-\pi$ and π we fix the phase shift as $\Delta\phi_i \in [-\pi, \pi)$.

By taking advantage of the periodic boundary conditions it can be easily shown that the sum of all phase shifts at any time moment is a multiple of 2π:

$$\sum_{i=1}^{N} \Delta\phi_i(t) = \sum_{i=1}^{N} (\phi_i(t) - \phi_{i-1}(t)) - 2\pi \sum_{i=1}^{N} \left\lfloor \frac{\phi_i(t) - \phi_{i-1}(t) + \pi}{2\pi} \right\rfloor = 2m(t)\pi. \tag{2.8}$$

The m, integer parameter is called winding number. Since $\Delta\phi_i$ is bounded, it can be shown, that the winding number is also has lower and upper bounds:

$$\left\lceil -\frac{N}{2} \right\rceil \leq m(t) < \left\lfloor \frac{N}{2} \right\rfloor , \tag{2.9}$$

where $\lceil x \rceil$ is the ceiling function, which evaluates to $-N/2$, if N is even and $-(N-1)/2$, if N is odd, while $\lfloor x \rfloor$ is the floor function evaluating to $N/2$ if N is even and $(N-1)/2$, if N is odd. Rewriting Eq. (2.4) in terms of the $\Delta\phi$ phases shifts we get the following condition for class (a) states:

$$\Delta\phi_{i+1} = \Delta\phi_i \, . \tag{2.10}$$

In this class all the phase shifts are the same thus the indices can be dropped, namely $\Delta\phi_i = \Delta\phi$. Consequently, using the winding number the possible values of $\Delta\phi$ can be easily determined[38,40,42,43]:

$$\Delta\phi = \frac{\Delta_N}{N} = 2\frac{m}{N}\pi\,. \tag{2.11}$$

Time dependencies are dropped, indicating the stationarity of the state. The consequence of such a condition is that these (a) type states can be characterized by only one parameter, which is the m winding number. Taking into account that all phase shifts are equal, the classical in-phase synchrony is member of this class, having $m = 0$. Anti-phase synchrony corresponds to the case of $\Delta\phi = -\pi$, thus its winding number is $m = -N/2$. Every other twisted or wave-like state will get the remaining indices. Results on linear stability shows that the only stable states are these case (a) states, thus we focus only on these patterns. In the terms of the winding number these states are stable if:

$$-\frac{N}{4} < m < \frac{N}{4}\,, \tag{2.12}$$

or in the terms of the phase shift:

$$-\frac{\pi}{2} < \Delta\phi < \frac{\pi}{2}. \tag{2.13}$$

In all other cases this type of state is unstable.

Since the remaining two classes are not stable we do not go into details concerning these unstable states.

2.2 Dynamics and final state prediction

The previous section revealed that the only attractors are type (a) states with winding numbers $-N/4 < m < N/4$. A first possible look on the dynamical aspects of such attractors would be to study their basins of attraction. The attraction basins of an attractors the collection of all points from where the system will converge to the given attractor. Numerical integration of Eq. (2.1) can be easily used to determine the relative size of the attraction basins by considering a large ensemble of random initial states and recording the number of appearance of each attractor. The outcome of such computer experiment is visible on Fig. 2.2. Results show that the distribution of the relative sizes of the attraction domains falls below a Gaussian envelope curve, centered around the state of in-phase synchrony. The standard deviation of the basin sizes scales linearly with the square root of the system size[40,43].

For studying the self-organization process we generalized the complex order parameter introduced by Kuramoto.[9] This yields a more general set of order parameters, each one linked to one of the m states:[34]

$$r_m(t)\mathrm{e}^{i\psi_m(t)} = \frac{1}{N}\sum_{j=1}^{N}\mathrm{e}^{i[\theta_j(t)-(j-1)\frac{2m\pi}{N}]}. \tag{2.14}$$

Similarly to the original order parameter, here each m state will have its own parameter, ranging in absolute value from 0 to 1. It can be shown that if the system approaches asymptotically to a state with

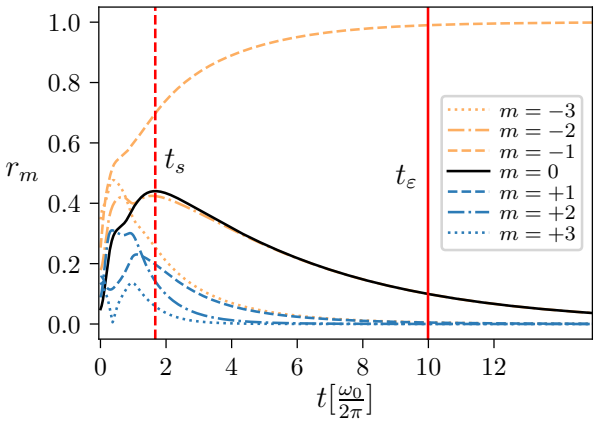

Figure 2.3: Time evolution of r_m order parameters. The number of oscillators is $N = 30$, however order parameters with $|m| \geq 4$ are not shown to avoid overcrowding of the graph. The vertical lines indicate the time moment of predictions with two different method. The t_s is linked to the derivatives of r_m, while t_ε corresponds to the crossing of the threshold value as in Eq. (2.15).

winding number m^*, its order parameter r_{m^*} will approach 1, while all other $r_{m \neq m^*}$ parameters will vanish.

Based on the time evolution of the order parameters a straightforward method of prediction would be to define an $\varepsilon > 0$ tolerance and check if one of the order parameters approach 1 within this tolerance. For small enough ε on can conclude that the state with the specific m will be selected. This assumption is equivalent to the following conjecture:

$$\text{if} \quad r_{m^*}(t) > 1 - \varepsilon \quad \Rightarrow \quad \lim_{t \to \infty} r_{m^*}(t) = 1. \tag{2.15}$$

The $1 - \varepsilon$ quantity is also referred to as threshold.

On Fig. 2.3 we present a sample time evolution of the order parameters. For illustration purposes we marked the time moment t_ε of passing the 0.99 threshold with a continuous vertical line. This value is high enough to consider the final state selected, so the prediction is correct, however this results in waste of CPU time since we set the threshold too high. Because r_m is bounded between 0 and 1 these values can only be reached by constant decrease and increase, respectively. As a conclusion in the exponential relaxation stage only one order parameter is increasing and the others decrease. Hence there must be a t_s time moment in the dynamics after which only the order parameter of the selected m^* state keeps increasing:

$$\begin{aligned} \dot{r}_{m*}(t \geq t_s) &> 0 \\ \dot{r}_{j \neq m^*}(t \geq t_s) &< 0\,. \end{aligned} \tag{2.16}$$

This time moment is marked by a vertical dashed line on Fig. 2.3. Based on the previous arguments we propose another prediction method by inverting the reasoning: we consider an m^* state to be selected if the only increasing order parameter is r_{m^*}.

This second method is inherently ill-defined, since the reverse argument may not necessarily be true and this will inevitably lead to false predictions. This indeed happens and it is caused by the type (c) saddle

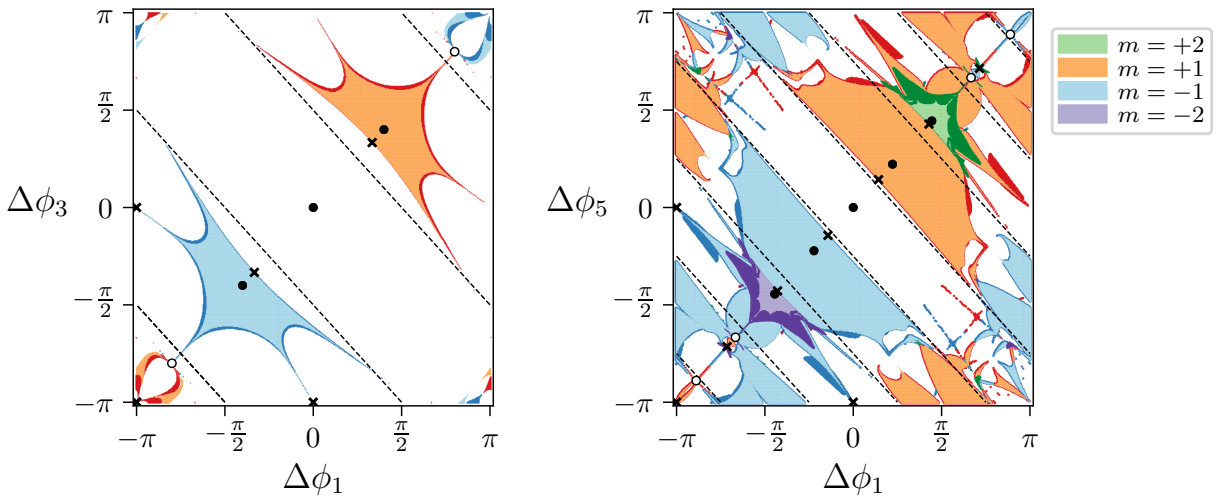

Figure 2.4: Cross section of the attraction basins for $N = 5$ (left) and $N = 9$ (right) oscillators. Black dots indicate the stable type (a) states while open circles mark unstable ones. Crosses represent type (c) saddle points. White space marks the basin of the in-phase synchronization, while colored areas belong to higher modes. Bright colors indicate the basins obtained using a high threshold ($1 - \varepsilon = 0.999$) while darker tones of the same color indicate initial states where predictions based on the derivatives of r_m were incorrect.

points. Saddle points are able distort trajectories by being attractive from some directions. Approaching a fixpoint implies an exponential slowing down in the dynamics, resulting in a transient metastable behavior.

In order to visualize this anomaly we compared the reliability of the two prediction methods and mapped the results on cross sections of the $\Delta\phi$ phase space. Figure 2.4 shows the outcome of such experiment for different system sizes. The cross sections were constructed using the fact that $\Delta\phi$ space of an N dimensional system is actually $N - 1$ dimensional due the constraint on the sum of phase shifts in Eq. (2.8). Hence a two dimensional cross section can be constructed by varying two phase shifts and applying some other constraint to the remaining ones. The most simple example of constraint is to fix the remaining $N - 3$ (one phase shift is always calculated from the sum in Eq. (2.8)). However in order to see most of the stationary states an "oblique" cross section was considered having maximal symmetry along the main diagonal of the N dimensional hypercube. On each panel of Fig. 2.4 there are two cross sections on top of each other constructed differently. Areas with bright coloring are created using a very low tolerance ($\varepsilon = 0.001$) considered to be accurate, while dark colors mark the initial states where the method using derivatives gave different results compared to the control. As expected, unstable nodes (hollow circles) and saddles (stars) are on the boundaries of attraction basins and incorrect predictions flock together around the edges between two domains or in the vicinity of unstable states.

Apparently, the question of choosing the best prediction method boils down to a trade-off between speed and precision as presented on Fig. 2.5. The first method with a proper choice of the tolerance can eliminate any doubt concerning the time evolution, however in this limit the method does not predict

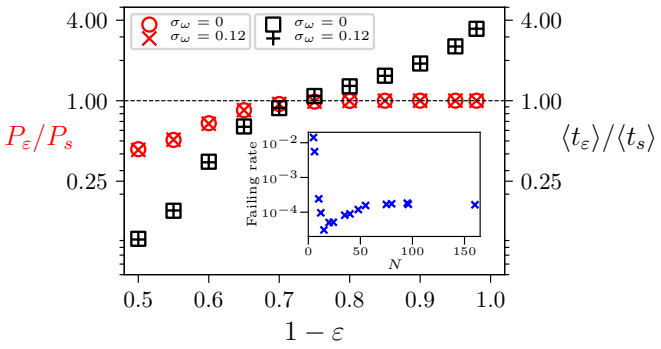

Figure 2.5: Benchmark of the two prediction methods. Red markers sign the comparison between the success rates of the fixed threshold (P_ε) and derivative (P_s) method as a function of the $1-\varepsilon$ threshold. Black markers correspond to the ratio of the average signaling time of the two methods $\langle t_\varepsilon\rangle$ and $\langle t_s\rangle$. The simulations were performed for inhomogeneous oscillators as well by considering a distribution of natural frequencies with nonzero σ_ω spread. $N = 18,\ K = 50$. The critical coupling for inhomogeneous case is $K_c = 42$.

but reassures results already visible to the naked eye. On the other hand, the second method is less time consuming, yet errors are inherently built in the method due to the deflections near saddles. The failing rate of this method (inset of Fig. 2.5) may seem statistically negligible however it will never become zero.

3

Rings of Kuramoto oscillators with time-delayed coupling

3.1 Symmetric phase locked states

The equations of motion we considered is a generalization of the system introduced in Eq. (2.1) by inserting a $\tau > 0$ time delay in the interaction kernel:

$$\dot{\theta}_i(t) = \omega_0 + K[\sin(\theta_{i-1}(t-\tau) - \theta_i(t)) + \sin(\theta_{i+1}(t-\tau) - \theta_i(t))]\,, \quad i = \overline{1, N}\,. \tag{3.1}$$

Notations are the same as in the non-delayed case and periodic boundary conditions are applied in order to maintain a ring-like topology. The introduction of time delay increased the number of free parameters of the system, however with a proper time rescaling one arrives to a set of dimensionless equations with three parameters including the system size N. Hence, we define the dimensionless time as $u = t/\tau$ and substitute in the equations of motion which leads to the following dimensionless system:

$$\frac{\mathrm{d}\theta_i(u)}{\mathrm{d}u} = \omega + \kappa[\sin(\theta_{i-1}(u-1) - \theta_i(u)) + \sin(\theta_{i+1}(u-1) - \theta_i(u))]\,, \tag{3.2}$$

with $\omega = \omega_0\tau$ being the dimensionless natural frequency and $\kappa = K\tau$ is the dimensionless coupling. The delay in this representation becomes unity.

Phase locked state is written in the form:

$$\theta_i(u) = \Omega u + \phi_i\,. \tag{3.3}$$

The final dimensionless frequency is denoted by Ω.

Type (a) states require $\phi_i - \phi_{i-1} = \Delta\phi$ to be constant over the system. Substituting this type of solution in Eq. (3.2) will give the following equation:

$$\Omega = \omega - 2\kappa\cos(\Delta\phi)\sin(\Omega)\,. \tag{3.4}$$

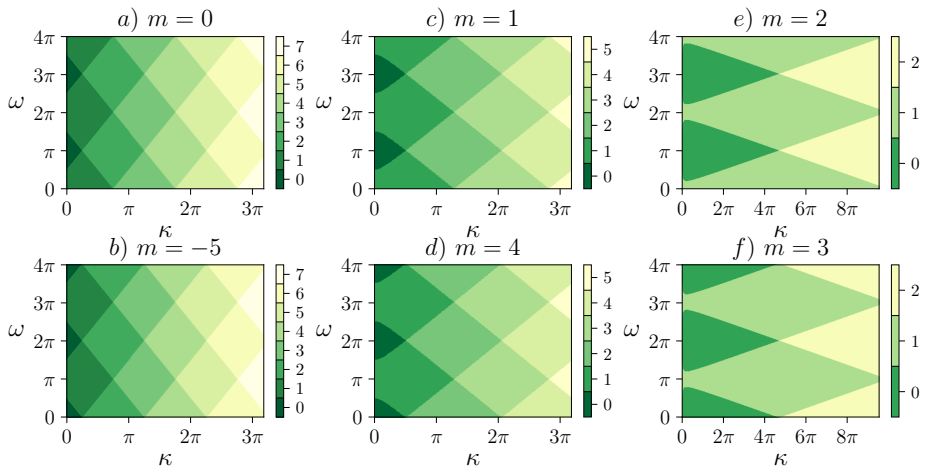

Figure 3.1: Number of stable Ω frequencies as a function of the ω natural frequency and κ coupling coded by colormaps. Zero stable Ω means that the state is unstable for the given parameter values. The winding numbers indicate the patterns we investigated, $\Delta\phi = 2m\pi/N$. Frequencies were obtained by solving Eq. (3.4), stability is determined using Eq. (3.6). The system size considered here is $N = 10$.

The $\Delta\phi$ phase shift has the same definition and meaning as described in Eq. (2.7). The condition on the sum of the phase shifts, namely $\sum_i \Delta\phi_i(t) = 2m(t)\pi$ still holds, since it is a consequence of the topology and not the dynamics. The equation from above is transcendental in Ω, however the exact value of Ω is important because in this case the phase shift alone is not enough to characterize a state, since there is more than one $\Delta\phi$ solution for a given $\Delta\phi$.

The stability analysis of such states involves the perturbation of solutions and studying the time evolution of the perturbation. The perturbation of the solutions is done in the following way:

$$\theta_i(u) = \Omega u + \varphi_i + \epsilon\,\eta_i(u)\,, \tag{3.5}$$

where $\epsilon \ll 1$. Using this ansatz we are able to determine the stability of the phase locked states by substituting them in the rescaled equations in Eq. (3.2).

Based on the work of Earl and Strogatz[44] it can be shown that in-phase synchrony states ($\Delta\phi = 0,\ m = 0$) are stable whenever $\cos(\Omega) > 0$, while anti-phase synchrony ($\Delta\phi = -\pi,\ m = -N/2$) is stable if $\cos(\Omega) < 0$. For states where m is neither 0 nor $-N/2$ the perturbation will lead to a system of linear DDEs, which we solved using the method of Asl and Ulsoy using the matrix Lambert W function[45]. A $\{\Omega, \Delta\phi\}$ state is stable if the real part of the following quantity is negative for a j values:

$$\lambda_j = W_0\left(2(\kappa_c\cos\frac{2\pi j}{N} + \mathrm{i}\kappa_s\sin\frac{2\pi j}{N})\mathrm{e}^{2\kappa_c}\right) - 2\kappa_c\,,\ j = \overline{0, N-1}, \tag{3.6}$$

where $\kappa_c = \cos(\Delta\phi)\cos(\Omega)$, $\kappa_s = \sin(\Delta\phi)\sin(\Omega)$ and W_0 is the principal branch of the Lambert W function.

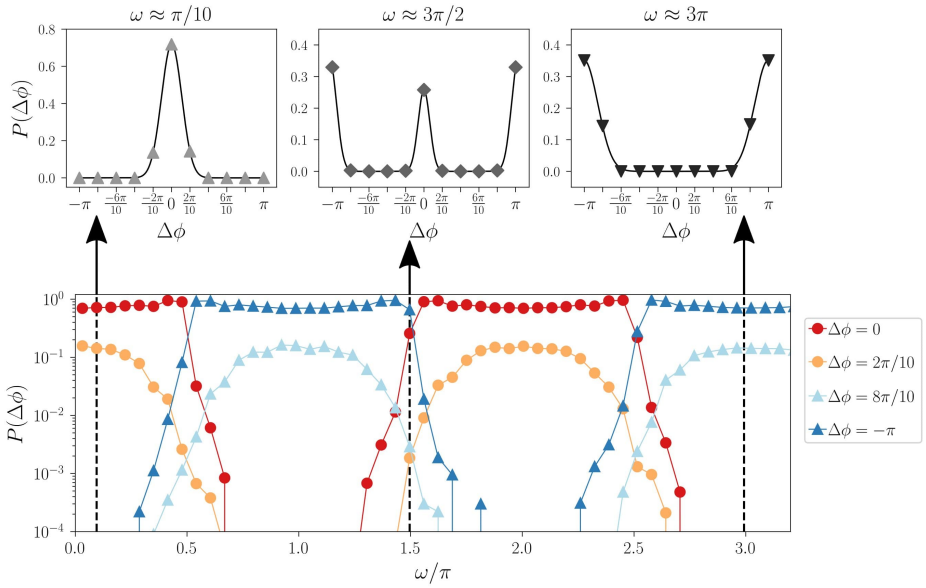

Figure 3.2: *Top*: Probability of detecting different phase locked state for different ω natural frequencies. *Bottom*: Probability of symmetric type (a) phase locked states as function of ω. Due to symmetric distributions only half of the probabilities are plotted. Dashed lines mark the parameters of the sample distributions of the top panel. $N = 10,\ \kappa = 2$. For each ω value an ensemble of 10^5 initial states were considered.

By evaluating λ in Eq. (3.6) we can construct the stability map of symmetric phase locked states in the $\omega - \kappa$ parameter space. First the possible Ω frequencies have to be determined for a given $\{m, \omega, \kappa\}$ set. Substituting these values in Eq. (3.6) will yield N exponents, or eigenvalues. In the case when all of them (except for the $j = 0$ case) are negative the frequency is stable. Such a set of stability maps is shown on Fig. 3.1 for different winding numbers.

3.2 Basins of attractions and bifurcations

Similarly to the non-delayed case we determined the size distribution of the attraction basins. Initialization in delayed systems is not a trivial question since instead of $\theta_i(0)$ values we need functions of $\theta_i(u),\ u \in [-1, 0)$ for each oscillator. Here we used "kick starting" meaning that we solve the uncoupled $\kappa = 0$ system for the initial $u \in [-1, 0)$ interval and interaction starts at $u = 0$. This setup is equivalent to in interaction with a finite speed of propagation. We note that the $\theta_i(-1)$ phases are still generated randomly form a uniform distribution over the $[0, 2\pi)$ interval. For detecting the final state we use the generalized order parameter defined in Eq. (2.14) with a high enough threshold. A sample for the basin size distributions is presented on the top panel of Fig. 3.2. Results show that changing the parameters can have very strong effects on the basin sizes opposed to the non-delayed case. The main difference compared to the non-delayed case is that probabilities may "flip" in a way that some states become practically undetectable due to the size of their attraction basin. The results of a more thorough analysis on the basin sizes is shown on the bottom panel of Fig. 3.2. As it was suggested by this sample, the basin sizes

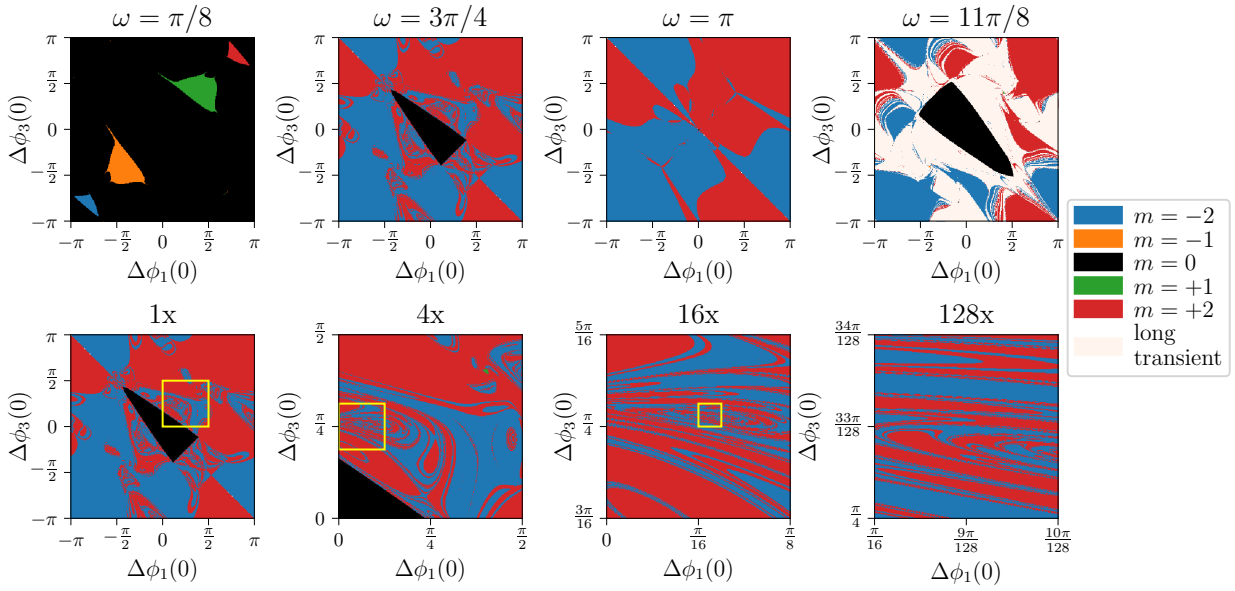

Figure 3.3: Two dimensional projections of cross sections showing the structure of the attraction basins in the $\Delta\phi_i(0)$ space for a system of $N = 5$ oscillators with coupling $\kappa = 2$ and varying natural frequency ω. *Top row:* The attraction basins have compact structure with simply connected boundaries for $\omega = \pi/8$ and $\omega = \pi$. Dominant states may vary as ω changes (see the color code in the legend). Fractal-like patterns can appear as well, for example at $\omega = 3\pi/4$ and $\omega = 11\pi/8$. These regions show a high degree of statistical self similarity (see bottom row for the blowups). Initial states developing into long term ($u \sim 10^5 - 10^6$) transient dynamics may appear as well in the cross sections, without converging towards one of the phase locked states. Each cross section is considered on grid of 320 by 320 initial states. *Bottom row:* Blowups of the cross section for $\omega = 3\pi/4$. The frames mark the sections that are enlarged on the graph on its right. Linear magnification rates compared to the original (1x) are given on the top of each plot.

can drastically change as ω is varied. Attraction basins can shrink and grow in size over four orders of magnitude. A typical periodic behavior is also present: for constant coupling the most probable state is either in-phase or anti-phase synchronization dictated by ω. We note that this behavior is not caused by the stability of these states because there is always at least one stable Ω frequency for each state(compare Fig. 3.1).

Results of Fig. 3.2 delivers a global overview of the interesting behavior of the attraction basins, however it does not provide any information about the spatial structure of these domains. To make a step further one can make an attempt to partition the phase space of the system into attraction basins. Using a similar workaround as in the case of Fig. 2.4 we considered a system of $N = 5$ oscillators. Such representative cross sections are presented on the top panel of Fig. 3.3 for different ω values. The first and the third cross section ($\omega = \pi/8$ and $\omega = \pi$) depicts a case of compact domains with simply connected basin boundaries. For $\omega = 3\pi/4$ and $\omega = 11\pi/8$ however there are regions resembling fractal-like structures with statistical self similarity. In order to investigate the aspects of these regions on the bottom panel of Fig. 3.3 we gradually enlarged these sections, proving that this type of statistical self similarity persists over at least three orders of magnitude. Another interesting finding is the appearance of long-

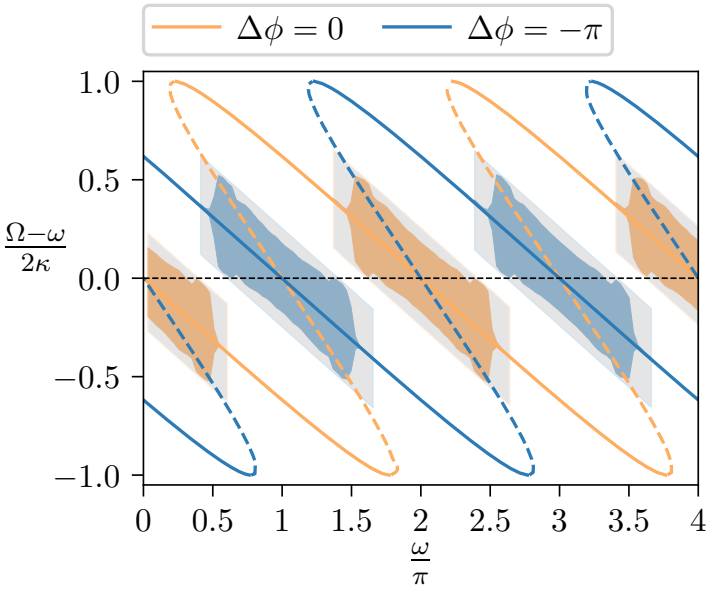

Figure 3.4: Bifurcation diagram of different Ω frequencies for in-phase and anti-phase synchrony as a function of dimensionless natural frequency ω. Stable frequencies are marked with continuous lines, while unstable frequencies are drawn with dashed curves. The horizontal dashed black line corresponds to the case of $\Omega = \omega$. The width of shaded areas correspond to the probability of observing the given frequencies. Width of gray areas mark probability 1, while no gray shading means that the frequency was not observed. $N = 10,\ \kappa = 2$.

term ($u \sim\ 10^5 - 10^6$ at least) seemingly non-vanishing transient behavior, which is very different from the discussed phase-locked states, since during this long periods of time no order parameter crosses the desired threshold value

Up to now the different Ω frequencies for the same phase locked patterns were neglected as we concentrated only on the phase shifts by using the order parameter in our simulations. In order to understand the multistability in the Ω space we constructed a bifurcation diagram of the dominant in- and anti-phase synchronized states states on Fig. 3.4. For the parameters we considered ($\kappa = 2,\ \omega \in [0, 4\pi]$) both states have at least one stable frequency. The pattern in the probabilities matches the behavior presented on the bottom panel of Fig. 3.2, namely that the system changes its preference periodically towards in-phase and anti-phase synchrony as a function of ω. For a given $\Delta\phi$ always the same Ω is selected even if there are multiple possibilities. When there are more stable frequencies for a pattern the system prefers the state with the frequency closest to its natural frequency. For a more quantitative reasoning valid also for other patterns as well we introduce two new parameters. First δ, which is proportional to the $\Omega - \omega$ difference:

$$\delta = \cos(\Delta\phi)\sin(\Omega)\,. \tag{3.7}$$

The second one is σ which refers to the symmetry of the pattern:

$$\sigma = \sin(\Delta\phi)\cos(\Omega)\,. \tag{3.8}$$

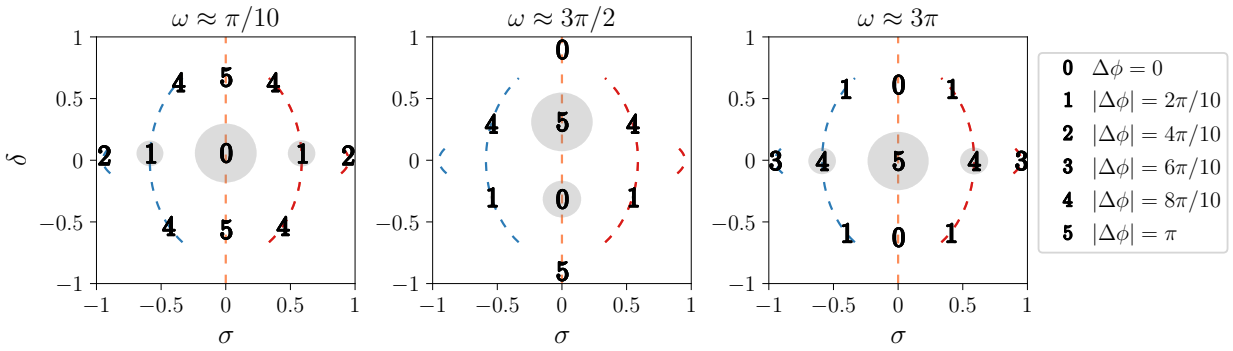

Figure 3.5: Stable Ω frequencies for different states in the $\delta - \sigma$ plane for different ω values. Numbers correspond to the absolute value of the winding number. Dashed lines and curves mark the path of $\Omega(\delta, \sigma)$ for a given m as the natural frequency ω changes. The areas of the gray circles is proportional to the basin size of a particular $\{\Delta\phi, \Omega\}$ state. Note that in the middle plot $\delta(|m| = 5) \approx \delta(m = 0)$, however a small change in δ can result in great differences in probabilities (see Fig. 3.2). $N = 10,\ \kappa = 2$.

This type of symmetry refers to the equality of the sine terms in Eq. (3.2) in the stationary states, namely $\sigma = \sin(-\Delta\phi_{i,i-1} - \Omega) - \sin(\Delta\phi_{i+1,i} - \Omega)$ This symmetry parameter is 0 (totally symmetric) for in-phase and anti-phase synchronization, while $|\sigma| > 0$ for other patterns.

As presented on Fig. 3.5 the interplay between σ and δ correlates with the change of the basin size distributions

The conclusions from the patterns on Fig. 3.5 can be reformulated as a set of simple heuristic guidelines explaining the selection process of final states:

- First, the selected state tends to be symmetric as possible, which explains why the peak of the basin size distributions are always around 0 and $-\pi$.
- If there are more solutions with the same $|\sigma|$ value, the one with the smaller $|\delta|$ will be preferred (see for example the $\sigma = 0$ line).
- Final states having the same $|\sigma|$ and $|\delta|$ are equally probable.

These observations suggest that calculation of δ and σ can help us in the estimation of the relative basin sizes for an ensemble of randomly initialized states.

3.3 Non-fixpoint type patterns

Without delay locally coupled oscillator rings are gradient systems. This means that the only allowed equilibria are fixpoints (i.e. phase locked states) and no other type of attractors, such as limit cycles or chaotic attractors can appear. In the case of delayed systems, the situation however is very different. First of all systems like Eq. (3.2) can not be easily reformulated as gradient system, since the future states depend not only on the present. This way we can not rule out the existence of more complex behavior. Furthermore the dependence on past configurations increases the dimensionality of the problem, also suggesting that there may be other emergent states as well besides phase locking.

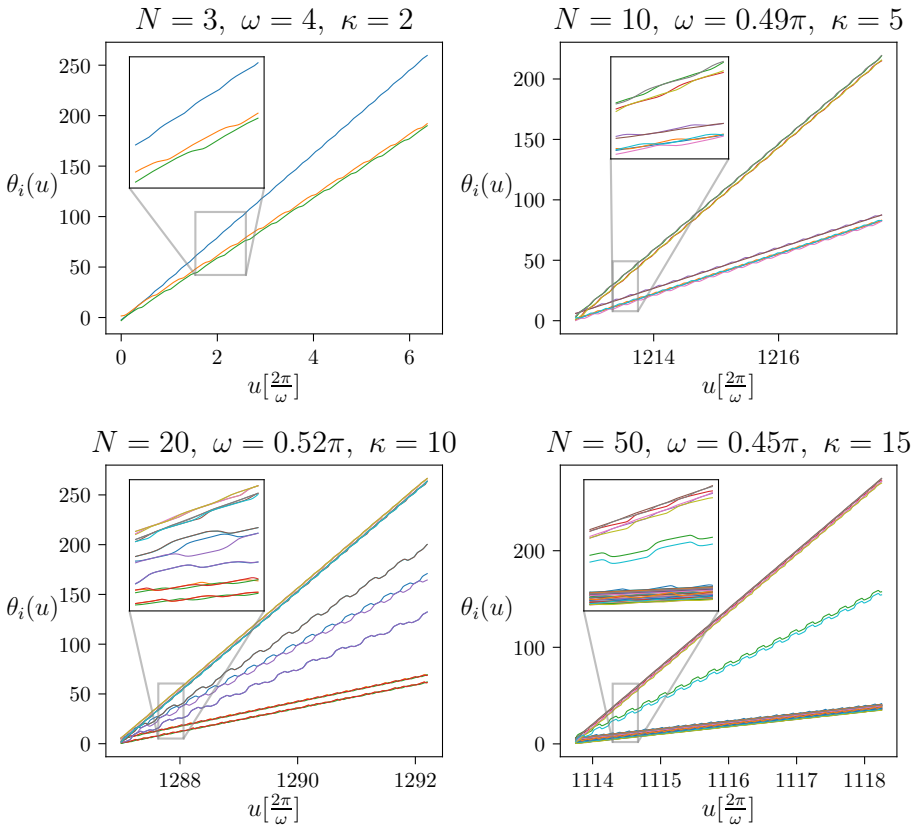

Figure 3.6: Time evolution of the $\theta_i(u)$ phases for different system sizes proving the existence of non trivial ordering besides phase locking. Due to the translational symmetry all phases have been rescaled between 0 and 2π then were let to evolve.

Even though the topic of this thesis is the emergence of phase locked patterns, the possibility of other behavior should not be overlooked. In this section we share our observations gained through computer simulations related to non-fixpoint patterns appearing in time delayed Kuramoto rings. Sticking to the main focus of our study the presentation will be a purely descriptive one, dedicated mainly to offer new research ideas and to raise interesting questions rather than explaining every aspect of these novel states.

The generalized order parameter in Eq. (2.14) is designed to indicate the convergence to one of the symmetric phase locked states, it is not well suited to search for any other type of attractors. The lack of convergence however, might be a hint that ordering may take different forms as well. The key factor here is the time scale, which we use as a proxy for identifying non-fixpoint pattern formations. A sufficiently long transient phase ($u \sim 10^5 - 10^6$) might suggest a different kind of ordering.

On Fig. 3.6 we show four representative time series of the θ_i phases for different system sizes. The first difference opposed to phase locked states is that the angular frequencies are not constant in time, however the oscillations seem to be periodic. There is also a clearly visible average frequency for each oscillator that leads to the overall increasing trends in the phases. Interestingly, these average frequencies can be the same for some of oscillators, thus forming groups with same average angular velocity. The

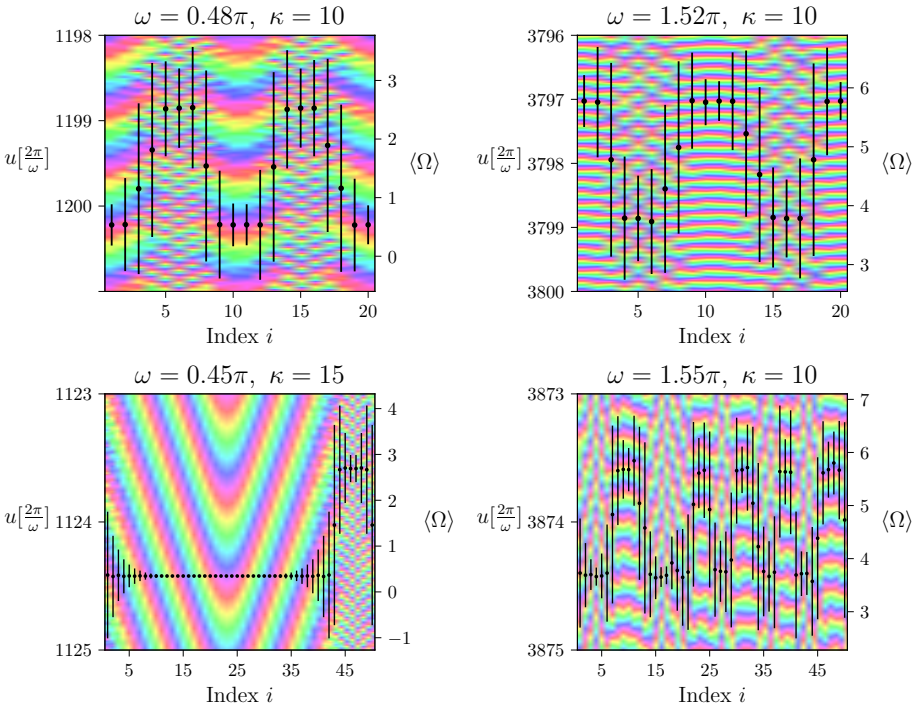

Figure 3.7: Space time plots of systems with $N = 20$ (top row) and $N = 50$ (bottom row) oscillators exhibiting clustering of oscillators with same average frequency. The phase at time u (left vertical axis of the graphs) is indicated by the rainbow color code. Average frequencies (right vertical axis of the graphs) are represented by black dots, while error bars refer to the standard deviation of the instantaneous frequency.

presence of such behavior in small and middle sized systems as well suggests that this phenomenon is not a consequence of the growing system size, but it has to be caused by the time delayed interaction.

In order to get a more detailed picture of this complex behavior it is important to study the emerging patterns as well. The so called space-time plots serve exactly this purpose where the state of the oscillators is presented in time and space as well by a color code. Such a plot is visible on Fig. 3.7. Above the phase representation the average frequencies are also plotted which reinforces the finding that oscillators with similar average frequencies tend to form spatial clusters. Error bars indicating the standard deviation of the frequency also show that the variability of the frequency tends to be greater at the borders between domains with similar $\langle\Omega\rangle$. The coexistence of regions with different patterns might suggest chimera states, however as it can be seen, all regions are ordered, or at least they show similar periodic behavior. This behavior can be a sign of a closed periodic orbit.

4
Conclusions & Outlook

In this thesis we have focused on the formation of phase locked patterns in locally coupled one dimensional Kuramoto systems. The phenomenon of phase locking, where oscillators end up having the same frequencies and consequently constant phase shifts between them, is not a new type of complex behavior in such systems. Therefore, the purpose of this work was to investigate the problem from a new viewpoint, namely predictability of final patterns and influence of model parameters on their basins of attraction.

In the first half of the thesis we presented our results on a simple locally coupled system of homogeneous Kuramoto oscillators. Inspired by past studies we developed a theoretical framework that we then used through all the thesis. Using this framework we have reproduced and completed recent results on such systems. The novel aspect of our investigation was the prediction of final states from a randomly initialized setup. We have generalized the complex Kuramoto order parameter and applied it to the time series of the oscillators. Results show that random initial states require a certain transient time period after which the long term behavior is clearly predictable. Two distinct prediction methods were introduced, both based on the generalized order parameter. These methods were compared in their precision and time efficiency, showing a trade off between these two properties. The effect of saddles and unstable nodes on the dynamics of the oscillators was discussed, revealing that trajectories can be heavily distorted around these repellers and basin boundaries as well. This type of distortions will inevitably lead to prediction errors. In the second part we took a step further by introducing time delayed interaction in one dimensional systems of homogeneous Kuramoto oscillators. The main problems we have investigated concerned the influence of the delay on the dynamics and the stable attractors of the oscillator ensemble. According to our observations this change can have drastic consequences under given circumstances. By these circumstances we mean different regions of the parameter space. The first major consequence is the that each phase locked pattern can be locally stabilized or destabilized, a very different behavior compared to the non-delayed case where the stability of the state is ultimately determined by the main properties of the state and not the parameters. As it has been advocated before, the attraction basin sizes can help us refine the picture on attractors and repellers obtained by studying their local stability, thus we studied them

with great interest. In this regard the parameters also proved to be the decisive factor. More precisely, the size of attraction basins can vary over several orders of magnitude depending on the parameters, meaning that some otherwise locally stable states become practically unobservable given the initializations we have used. It seems that intrinsic frequencies play an important role in this peculiar behavior observed in the basin sizes. Another important difference compared to non-delayed systems is the appearance of closed orbits discussed in more detail in Section 3.3, which could be interpreted as limit cycles or even chimera states.

The Kuramoto model have become a prototype model in the study of spontaneous synchronization and other types of complex behavior. It was proven to be helpful in a wide range of interdisciplinary problems, thus becoming a fundamental tool in the field of complex systems. The literature covering the usage of the model is vast, pointing far beyond the concept of frequency entrainment in globally coupled oscillator systems, the initial topic which Kuramoto and Nishikawa had developed the model for. For such a fundamental model it is hard to discover new results however, key models need to be understood profoundly, meaning that besides broadening its applicability, one should also strive for deepening our knowledge, by questioning the fundamentals. The present work fits in this line of studies, by taking another look on previously discussed problems.

Publications related to the thesis

ISI publications

- Károly Dénes, Bulcsú Sándor, and Zoltán Néda. Pattern selection in a ring of Kuramoto oscillators, *Communications in Nonlinear Science and Numerical Simulation*, 78:104868, 2019. IF=4.115

- Károly Dénes, Bulcsú Sándor, and Zoltán Néda. On the predictability of the final state in a ring of Kuramoto rotators, *Romanian Reports in Physics*, 78:108, 2019. IF=1.84

- Károly Dénes, Bulcsú Sándor, and Zoltán Néda. Synchronization patterns in rigs of time-delayed Kuramoto oscillators. *Communications in Nonlinear Science and Numerical Simulation*, 93:105505, 2021. IF=4.115

Conferences

1. Károly Dénes, Bulcsú Sándor, and Zoltán Néda (6-10 June 2016). *Collective behavior patterns in a ring of Kuramoto-type rotators with time-delay*. [Oral presentation]. XXXVI. Dynamics Days Europe, Corfu, Greece.

2. Károly Dénes, Bulcsú Sándor, and Zoltán Néda (10-14 July 2017). *Kuramoto oscillators in a ring-like topology*. [Poster presentation]. SigmaPhi2017, International Conference on Statistical Physics, Corfu, Greece.

3. Károly Dénes, Bulcsú Sándor, and Zoltán Néda (19-23 March 2018). *Pattern selection in a ring of Kuramoto rotators*. [Poster presentation]. Analysis and Modeling of Complex Oscillatory Systems, Barcelona, Spain.

4. Károly Dénes, Bulcsú Sándor, and Zoltán Néda (1-4 May 2018). *Collective modes of identical Kuramoto rotators in a ring-like topology*. [Poster presentation]. MECO43: 43rd Conference of the Middle European Cooperation in Statistical Physics, Kraków, Poland.

5. Károly Dénes, Bulcsú Sándor, and Zoltán Néda (14-17 June 2018). *Collective modes of identical Kuramoto rotators in a ring-like topology*. [Oral presentation]. 12th Joint Conference on Mathematics and Computer Science, Cluj-Napoca, Romania.

6. Károly Dénes, Bulcsú Sándor, and Zoltán Néda (2-6 September 2019). *Bifurcations in systems of Kuramoto oscillators with delayed coupling*. [Poster presentation]. XXXIX. Dynamics Days Europe, Rostock, Germany.

7. Károly Dénes, Bulcsú Sándor, and Zoltán Néda (14-16 September 2020). *Stabilizing phase-locked patterns in systems of Kuramoto oscillators with delayed coupling*. [Poster presentation]. MECO45: 45th Conference of the Middle European Cooperation in Statistical Physics - online, Cluj-Napoca, Romania

Selected references

[1] Steven Strogatz. *Sync: The emerging science of spontaneous order*. Penguin UK, 2004.

[2] D Attenborough. BBC Trials of Life Talking to Strangers, 1990.

[3] Charles S Peskin. Mathematical aspects of heart physiology. *Courant Inst. Math*, 1975.

[4] Kurt Wiesenfeld, Pere Colet, and Steven H Strogatz. Synchronization transitions in a disordered Josephson series array. *Physical review letters*, 76(3):404, 1996.

[5] Pat Dallard, AJ Fitzpatrick, A Flint, S Le Bourva, A Low, RM Ridsdill Smith, and M Willford. The London Millennium footbridge. *Structural Engineer*, 79(22):17–21, 2001.

[6] C Huygens. Letter to de sluse. letter no. 1333 of february 24, 1665. *Oeuvres Complète de Christiaan Huygens. Correspondence*, 5:1664–1665, 1665.

[7] Steven H Strogatz. Norbert Wiener's brain waves. In *Frontiers in mathematical biology*, pages 122–138. Springer, 1994.

[8] Arthur T. Winfree. Biological rhythms and the behavior of populations of coupled oscillators. *Journal of Theoretical Biology*, 16(1):15 – 42, 1967.

[9] Yoshiki Kuramoto. Self-entrainment of a population of coupled non-linear oscillators. In Huzihiro Araki, editor, *International Symposium on Mathematical Problems in Theoretical Physics*, volume 39 of *Lecture Notes in Physics*, pages 420–422. Springer Berlin Heidelberg, 1975.

[10] Steven H Strogatz and Renato E Mirollo. Stability of incoherence in a population of coupled oscillators. *Journal of Statistical Physics*, 63(3-4):613–635, 1991.

[11] Steven H Strogatz, Renato E Mirollo, and Paul C Matthews. Coupled nonlinear oscillators below the synchronization threshold: relaxation by generalized Landau damping. *Physical Review Letters*, 68(18):2730, 1992.

[12] Hidetsugu Sakaguchi, Shigeru Shinomoto, and Yoshiki Kuramoto. Local and grobal self-entrainments in oscillator lattices. *Progress of Theoretical Physics*, 77(5):1005–1010, 1987.

[13] Hidetsugu Sakaguchi, Shigeru Shinomoto, and Yoshiki Kuramoto. Mutual entrainment in oscillator lattices with nonvariational type interaction. *Progress of Theoretical Physics*, 79(5):1069–1079, 1988.

[14] Duncan J Watts and Steven H Strogatz. Collective dynamics of 'small-world' networks. *Nature*, 393(6684):440, 1998.

[15] Albert-László Barabási and Réka Albert. Emergence of scaling in random networks. *Science*, 286(5439):509–512, 1999.

[16] Hyunsuk Hong, Moo-Young Choi, and Beom Jun Kim. Synchronization on small-world networks. *Physical Review E*, 65(2):026139, 2002.

[17] Hyunsuk Hong, Hyunggyu Park, and Lei-Han Tang. Finite-size scaling of synchronized oscillation on complex networks. *Physical Review E*, 76(6):066104, 2007.

[18] Carsten Grabow, Steven M Hill, Stefan Grosskinsky, and Marc Timme. Do small worlds synchronize fastest? *EPL (Europhysics Letters)*, 90(4):48002, 2010.

[19] S Yoon, M Sorbaro Sindaci, AV Goltsev, and JFF Mendes. Critical behavior of the relaxation rate, the susceptibility, and a pair correlation function in the Kuramoto model on scale-free networks. *Physical Review E*, 91(3):032814, 2015.

[20] Fumito Mori. Necessary condition for frequency synchronization in network structures. *Physical review letters*, 104(10):108701, 2010.

[21] Hiroaki Daido. Quasientrainment and slow relaxation in a population of oscillators with random and frustrated interactions. *Physical review letters*, 68(7):1073, 1992.

[22] Hidetsugu Sakaguchi and Yoshiki Kuramoto. A soluble active rotater model showing phase transitions via mutual entertainment. *Progress of Theoretical Physics*, 76(3):576–581, 1986.

[23] Seunghwan Kim, Seon Hee Park, and Chang Su Ryu. Nonequilibrium phenomena in globally coupled active rotators with multiplicative and additive noises. *ETRI journal*, 18(3):147–160, 1996.

[24] Shigeru Shinomoto and Yoshiki Kuramoto. Phase transitions in active rotator systems. *Progress of Theoretical Physics*, 75(5):1105–1110, 1986.

[25] Yoshiki Kuramoto and Dorjsuren Battogtokh. Coexistence of coherence and incoherence in nonlocally coupled phase oscillators. *arXiv preprint cond-mat/0210694*, 2002.

[26] Daniel M Abrams and Steven H Strogatz. Chimera states for coupled oscillators. *Physical review letters*, 93(17):174102, 2004.

[27] Aaron M Hagerstrom, Thomas E Murphy, Rajarshi Roy, Philipp Hövel, Iryna Omelchenko, and Eckehard Schöll. Experimental observation of chimeras in coupled-map lattices. *Nature Physics*, 8(9):658–661, 2012.

[28] Erik Andreas Martens, Shashi Thutupalli, Antoine Fourrière, and Oskar Hallatschek. Chimera states in mechanical oscillator networks. *Proceedings of the National Academy of Sciences*, 110(26):10563–10567, 2013.

[29] Tomasz Kapitaniak, Patrycja Kuzma, Jerzy Wojewoda, Krzysztof Czolczynski, and Yuri Maistrenko. Imperfect chimera states for coupled pendula. *Scientific reports*, 4:6379, 2014.

[30] Lucia Valentina Gambuzza, Arturo Buscarino, Sergio Chessari, Luigi Fortuna, Riccardo Meucci, and Mattia Frasca. Experimental investigation of chimera states with quiescent and synchronous domains in coupled electronic oscillators. *Phys. Rev. E*, 90:032905, Sep 2014.

[31] Jerzy Wojewoda, Krzysztof Czolczynski, Yuri Maistrenko, and Tomasz Kapitaniak. The smallest chimera state for coupled pendula. *Scientific reports*, 6(1):1–5, 2016.

[32] Vincenzo Nicosia, Miguel Valencia, Mario Chavez, Albert Díaz-Guilera, and Vito Latora. Remote synchronization reveals network symmetries and functional modules. *Physical review letters*, 110(17):174102, 2013.

[33] Y. Qin, Y. Kawano, and M. Cao. Stability of remote synchronization in star networks of kuramoto oscillators. In *2018 IEEE Conference on Decision and Control (CDC)*, pages 5209–5214, 2018.

[34] Károly Dénes, Bulcsú Sándor, and Zoltán Néda. Pattern selection in a ring of Kuramoto oscillators. *Communications in Nonlinear Science and Numerical Simulation*, 78:104868, 2019.

[35] Károly Dénes, Bulcsú Sándor, and Zoltán Néda. On the predictability of the final state in a ring of Kuramoto rotators. *Romanian Reports in Physics*, 71:108, 2019.

[36] Károly Dénes, Bulcsú Sándor, and Zoltán Néda. Synchronization patterns in rings of time-delayed Kuramoto oscillators. *Communications in Nonlinear Science and Numerical Simulation*, 93:105505, 2021.

[37] J. Ochab and P. F. Gora. Synchronisation of coupled oscillators in a local one-dimensional Kumamoto model. In Lawniczak, AT and Makowiec, D and Di Stefano, BN, editor, *Summer Solstice 2009, International Conference on Discrete Models of Complex Systems*, volume 3 of *Acta Physica Polonica B Proceedings Supplement*, pages 453–462, 2010.

[38] T. K. Roy and A. Lahiri. Synchronized oscillations on a Kuramoto ring and their entrainment under periodic driving . *Chaos, Solitons & Fractals*, 45(6):888 – 898, 2012.

[39] Xia Huang, Meng Zhan, Fan Li, and Zhigang Zheng. Single-clustering synchronization in a ring of Kuramoto oscillators. *Journal of Physics A: Mathematical and Theoretical*, 47:125101, 03 2014.

[40] Daniel A. Wiley, Steven H. Strogatz, and Michelle Girvan. The size of the sync basin. *Chaos: An Interdisciplinary Journal of Nonlinear Science*, 16(1):015103, 2006.

[41] Morris W Hirsch, Stephen Smale, and Robert L Devaney. *Differential equations, dynamical systems, and an introduction to chaos*. Academic press, Boston, 2012.

[42] Ramana Dodla, Abhijit Sen, and George L. Johnston. Phase-locked patterns and amplitude death in a ring of delay-coupled limit cycle oscillators. *Phys. Rev. E*, 69:056217, May 2004.

[43] Paulo FC Tilles, Fernando F Ferreira, and Hilda A Cerdeira. Multistable behavior above synchronization in a locally coupled Kuramoto model. *Physical Review E*, 83(6):066206, 2011.

[44] Matthew G. Earl and Steven H. Strogatz. Synchronization in oscillator networks with delayed coupling: A stability criterion. *Phys. Rev. E*, 67:036204, Mar 2003.

[45] Farshid Maghami Asl and A Galip Ulsoy. Analysis of a system of linear delay differential equations. *J. Dyn. Sys., Meas., Control*, 125(2):215–223, 2003.